Four-Photon Mixing and High-Speed WDM Systems

R. W. Tkach, *Member, IEEE,* A. R. Chraplyvy, Fabrizio Forghieri, *Member, IEEE,*
A. H. Gnauck, and R. M. Derosier

(Invited Paper)

***Abstract*—The trend toward higher bit rates in lightwave communications has increased interest in dispersion-shifted fiber to minimize dispersion penalties. At the same time optical amplifiers have increased interest in wavelength multiplexing. These two methods of increasing system capacity, if used together, can result in severe degradation due to fiber nonlinearity. This paper discusses the impact of the principal nonlinearity, four-photon mixing, and describes strategies that allow simultaneous use of high bit rates and WDM.**

I. Introduction

THE availability of efficient and powerful optical amplifiers has led to a resurgence of interest in wavelength multiplexing for lightwave systems, since erbium-doped fiber amplifiers can amplify many channels without significant crosstalk, and can provide several nm of optical bandwidth for transmission distances of hundreds to thousands of kilometers. At the same time, progress in electronics has made it possible to increase single-channel bit rates up to 10 Gb/s. The combination of such high speed channels with WDM offers capacities of over 100 Gb/s. To employ 10-Gb/s modulation over long distances requires low chromatic dispersion. For a 1000-km span the net chromatic dispersion must be below 1000 ps/nm, so that the transmission fiber must have dispersion below 1 ps/nm-km on average. In addition, to preserve adequate signal-to-noise ratio, a 10-Gb/s system operating over 1000 km with an amplifier spacing of 100 km requires 1 mw/channel [1]. Typically several dB of additional power are required for margins.

For WDM systems the simultaneous requirements of high launched power and low dispersion lead to the generation of new frequencies by four-photon mixing [2], [3]. These generated waves can interfere with system operation [4]–[7]. Inoue has proposed schemes to avoid this impairment, either by specialized modulation of the transmitted light [8], [9], or by devices introduced into the transmission line [10]. In this paper we describe the nature and size of the impairment due to four-photon mixing in lightwave systems, and describe two schemes which can ameliorate that impairment and have allowed us to demonstrate high-speed operation with WDM: unequal spacing of the channel frequencies and management of the fiber dispersion. These methods allow the use of conventional transmitters, and require no additional devices in the transmission line.

Manuscript received July 1, 1994.

The authors are with AT&T Bell Laboratories, Crawford Hill Laboratory, Holmdel, NJ 07733-0400 USA.

IEEE Log Number 9411020.

Four-photon mixing is a third-order nonlinearity in silica fibers, which is analogous to intermodulation distortion in electrical systems, so that in multichannel systems three optical frequencies mix to generate a fourth

$$f_g = f_i + f_j - f_k.$$

If we assume that the input signals are not depleted by the generation of mixing products, the magnitude of this new optical signal is given by (in esu) [11]

$$P_g = \frac{1024\pi^6}{n^4\lambda^2c^2}\left(\frac{D\chi_{1111}L_{eff}}{A_{eff}}\right)^2 P_iP_jP_ke^{-\alpha L}\eta \qquad (1)$$

where n is the refractive index, λ is the wavelength of the light, c is the speed of light, P_i, P_j, P_k are the input powers of the channels, L_{eff} is the effective length of the fiber, given by

$$L_{eff} = \frac{1}{\alpha}\left(1 - e^{-\alpha L}\right)$$

with α the fiber loss, here taken to be 0.2 dB/km. A_{eff} is the effective area of the fiber, $D = 3$ for two-tone products and 6 for three-tone products, and $\chi_{1111} = 4 \times 10^{-15}$ esu is the nonlinear susceptibility. The nonlinear susceptibility can be expressed in terms of the nonlinear index of refraction n_2, in the case of a single polarization, as

$$\chi_{1111}[esu] = \frac{cn^2}{480\pi^2}n_2[m^2/W].$$

The efficiency η is given by

$$\eta = \frac{\alpha^2}{\alpha^2 + \Delta\beta^2}\left(1 + \frac{4e^{-\alpha L}\sin^2(\Delta\beta L/2)}{(1 - e^{-\alpha L})^2}\right).$$

The quantity $\Delta\beta$ is the difference of the propagation constants of the various waves, due to dispersion, and for a two-tone product with channel spacing Δf, is given by

$$\Delta\beta = \beta_g + \beta_k - \beta_j - \beta_i = \frac{2\pi\lambda^2}{c}\Delta f^2\left(D + \Delta f\frac{\lambda^2}{c}\frac{dD}{d\lambda}\right)$$

where the dispersion D and its slope are computed at λ_k. This analysis has been extended to multiple amplified spans [12], [13].

For sufficiently low fiber chromatic dispersion $\Delta\beta \approx 0$ and $\eta \approx 1$. If in addition, all channels have the same power P_{in}, the ratio of the generated power P_g to the transmitted power of the channel P_{out} can be written as

$$\frac{P_g}{P_{out}} = \frac{1024\pi^6}{n^4\lambda^2c^2}\left(\frac{D\chi^{(3)}L_{eff}}{A_{eff}}\right)^2 P_{in}^2.$$

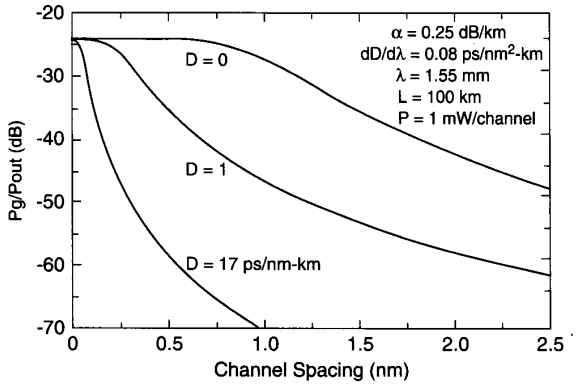

Fig. 1. Plot of the ratio of generated mixing-product power to transmitted channel power versus channel spacing for two equal-power channels. Curves are shown for three different values of fiber chromatic dispersion.

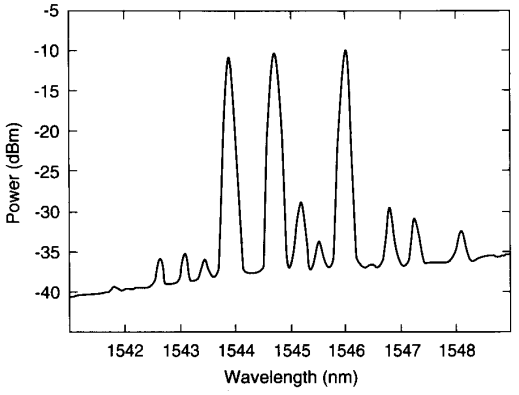

Fig. 2. Optical power spectrum measured at the output of a 25-km length of dispersion-shifted fiber ($D = -0.2$ ps/nm · km at the central channel) when three 3-mW channels are launched.

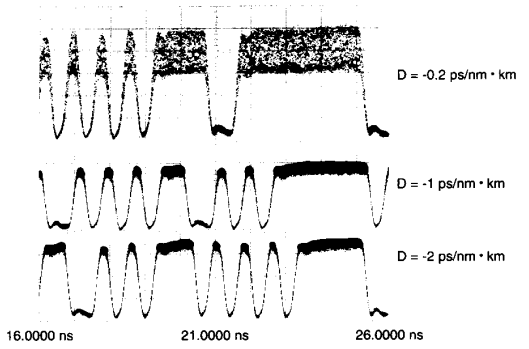

Fig. 3. Bit patterns observed for the central channel when the three channels are equally spaced so that the largest mixing product falls on the central channel. Shown for three different values of fiber chromatic dispersion. Launched power was 3 mW/channel.

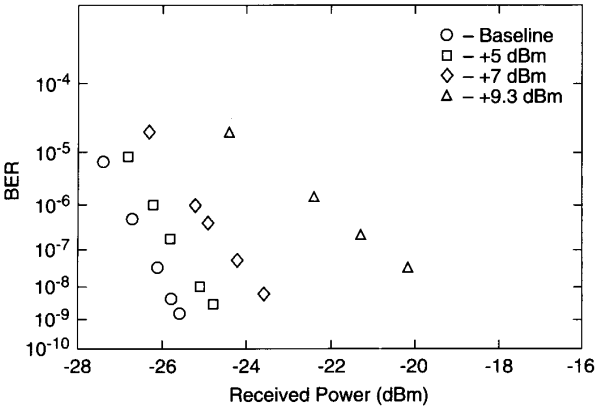

Fig. 4. Bit-error-ratio curves for the $D = -0.2$ ps/nm·km case at three different launched powers. Values quoted are for the total launched power of the three channels. Only the central channel was modulated at 2.5 Gb/s so that the interference is always present.

Note that the ratio of the generated power to the transmitted power scales with P_{in}^2. For the case of a three-tone product (D = 6) at 1.55 μm, with $L_{eff} = 22$ km, $A_{eff} = 55$ μm^2, this equation evaluates to give a mixing product to transmitted channel power ratio of $0.01 \times P_{in}^2[\mathrm{mW}^2]$. Fig. 1 shows the ratio of generated power to transmitted power for a two-tone product as a function of channel spacing for three different values of chromatic dispersion. Note that the top curve, which corresponds to a case where one of the two tones is coincident with the fiber zero-dispersion frequency, and the mixing product farthest from the zero-dispersion frequency is considered, maintains high efficiency for channel spacings as large as 1 nm. Of course the product on the other side of the channels is phase matched for all channel spacings in this case [14]. Fig. 2 shows a measured spectrum at the output of a 25-km dispersion-shifted fiber ($\lambda_0 = 1547.3$ nm) when three 3-mW signals are launched at the input. Nine new frequencies are observable with a peak ratio of 0.01 to the input signals. For N channels launched, the number of mixing products generated is

$$M = \frac{1}{2}(N^3 - N^2).$$

So for eight channels, 224 products are generated. Fig. 3 shows the effect on the bit pattern of the central channel in the experiment of Fig. 2 when the three channels are equally spaced. Fig. 4 shows bit-error-ratio curves for three input powers for this case. Clearly, even at these modest power levels and short system lengths, there is substantial impairment. The penalties observed in this experiment are exacerbated by a fixed decision threshold in the regenerator. Uniform spacing of the input channel frequencies causes the large product seen in Fig. 2 to fall at the same frequency as the central channel, and the resulting beating gives rise to the width of the "one" level. Thus, although the product itself has only 1% of the power of the channel, it results in a ± 1 dB fluctuation in the received power. Fig. 5 shows a histogram of the "one" level illustrating that the impairment in this case is a power penalty, since the distribution has well defined maximum and minimum values. For larger numbers of channels, many distributions like this one must be combined.

The large penalty resulting from relatively small mixing products in the case of equal channel spacing begs the question of unequal spacing. If the channels are arranged so that no mixing products fall on any of the channels, this parametric

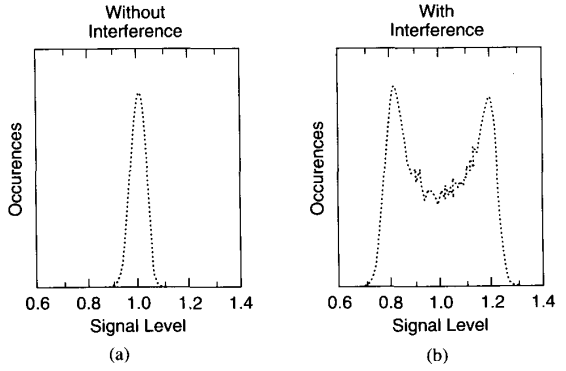

Fig. 5. Histograms taken at the sampling point of the marks both with and without the outside channels present for the $D = -0.2$ ps/nm·km case.

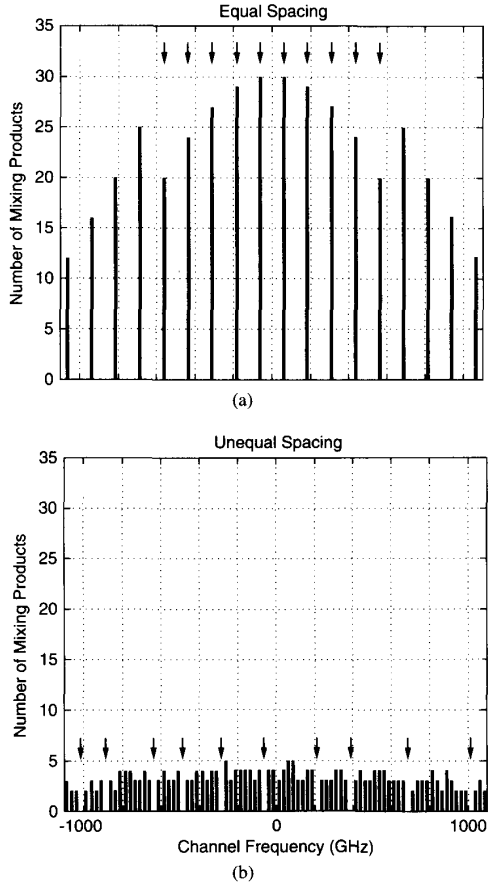

Fig. 6. Graphs showing the number of mixing products falling at various frequencies for a 10-channel system. (a) Equally spaced channels. (b) Unequally spaced channels. Arrows indicate the channel frequencies.

gain effect can be avoided. A method of determining such channel arrangements has been described [15], [16]. Since typical WDM systems use channel spacings large compared to the bandwidth of the signals, there is an opportunity to use this "wasted bandwidth" to place mixing products away from the channels. In systems with channels equally spaced in *wavelength*, the frequency spacing will not be uniform.

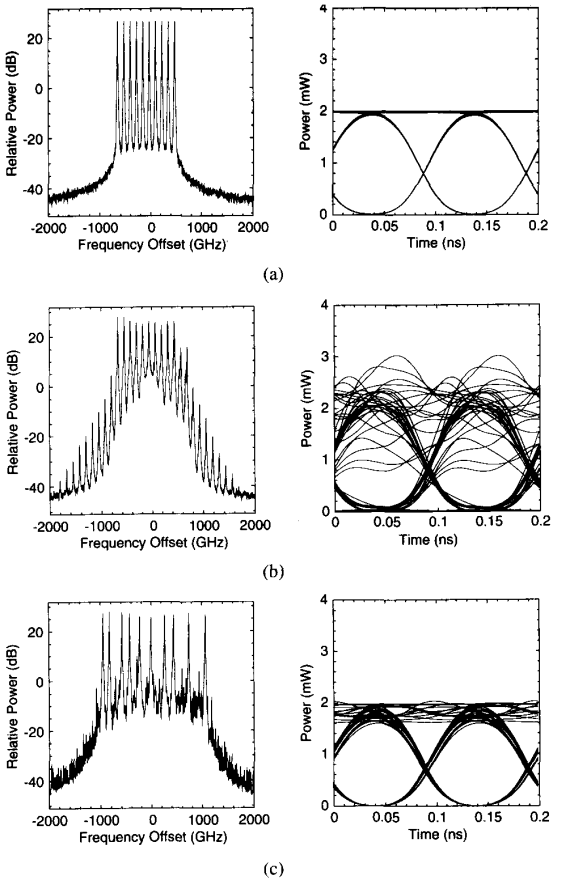

Fig. 7. Simulation results for the channel placements of Fig. 6. The system consists of 500 km of fiber with the dispersion zero located at zero Frequency Offset. Optical amplifiers are spaced every 50 km. The channels are modulated at 10 Gb/s and are launched into each span of fiber with 1 mW average power. (a) System input power spectrum and eye diagram. (b) System output, equally spaced channels. (c) System output, unequally spaced channels.

However, it is important to note that the unequal frequency spacing inherent in equal *wavelength* spacing is not sufficient to prevent interference. The difference in frequency spacing, and hence the offset of the mixing product from the channel, must be larger than the bit rate to avoid interference [15]. For the three-channel case of Figs. 3 and 4, the channel spacing would need to be 4 nm for the difference in frequency spacing to be 2.5 GHz. The requirement of no mixing product falling on any channel was shown to be equivalent to requiring that the difference between any two channel frequencies be unique, [15]. For reasonable numbers of channels such an arrangement can be found by an exhaustive computer search. Fig. 6 shows the number of mixing products at various frequencies for equal and unequal spacing for a 10-channel system, where the mixing products are offset from the channels by at least 25 GHz and the channels are separated by at least 1 nm. Fig. 7 shows a simulation for this case; the improvement in performance is obvious. The methodology of these simulations is described in detail below.

An experiment demonstrating this improved performance [17] is diagrammed in Fig. 8. Eight 10-Gb/s channels were

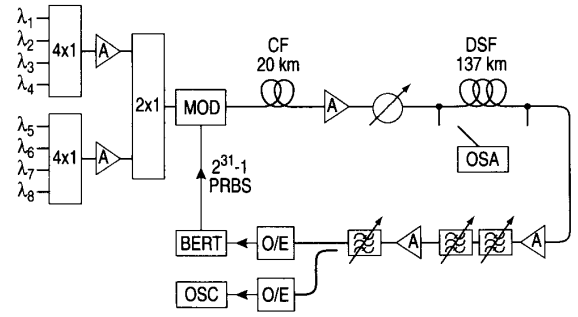

Fig. 8. Experimental diagram for a 137-km repeaterless transmission experiment with eight 10-Gb/s channels demonstrating the benefits of unequal channel spacing. The 20-km fiber after the modulator was conventional step-index fiber with 16 ps/nm · km chromatic dispersion and was used to decorrelate the bit patterns of the various wavelength channels prior to launching into the transmission fiber.

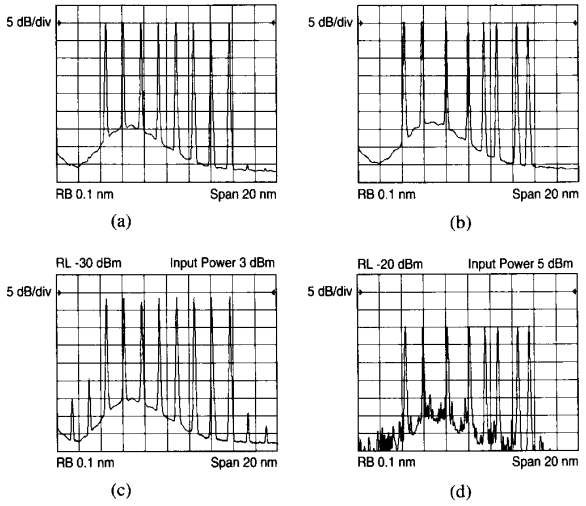

Fig. 9. Input and output spectra for the experiment of Fig. 8 for both equal and unequal spacing. (a) Equal spacing, input. (b) Unequal spacing, input. (c) Equal spacing, output. (d) Unequal spacing, output.

launched into 137 km of dispersion-shifted fiber. The zero-dispersion wavelength of the initial 40 km (the portion of the fiber relevant for the generation of mixing products) of the line fell midway between the second and third channels. The remaining spools of fiber had slowly decreasing zero-dispersion wavelengths. Input and output spectra are shown in Fig. 9 for both equal and unequal spacing. The total occupied bandwidth was the same in both cases. Fig. 10 shows the bit-error ratio as a function of launched power for both cases. Note that the equally spaced case has a minimum BER of 10^{-6}, while the unequally spaced case operates essentially error free from 2–6 dBm. The degradation setting in at 7 dBm arises from depletion of the channel power by the mixing products. Thus the unequally spaced system allows a 6–7 dB increase in launched power, but the generation of mixing products eventually degrades system performance.

While unequal spacing ameliorates the effects of mixing products on the performance of a WDM system, it is also possible to prevent the generation of those products in the

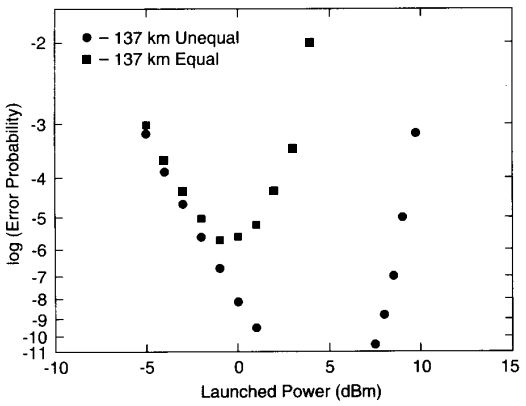

Fig. 10. Bit-error-ratio curves versus launched power per channel for both equal and unequal spacing.

first place by avoiding phasematching. Fig. 3 illustrates the effect of fiber chromatic dispersion on the mixing impairment. As can be seen, quite small values of dispersion (1–2 ps/nm · km) can have a dramatic effect. To avoid a dispersion penalty in a high-speed system, the requirement is that the total chromatic dispersion be low. If however, the local chromatic dispersion of the fibers can be controlled, one may retain low total chromatic dispersion while avoiding low dispersion in any fiber segment. This notion has been suggested previously, [18], [19].

Computer simulation allows various scenarios for dispersion management to be evaluated without actually constructing the transmission lines. The simulation begins by creating an electric field for each channel including laser linewidth as a random walk of the phase, and external modulation, modeled as a Mach-Zehnder modulator with variable chirp. The chirp parameter was set to zero for the work described here. The channels are then summed to give a net electric field input to the transmission fiber. Propagation is simulated by solving the nonlinear Schrodinger equation with a split-step algorithm, [20]. The step size is calculated at each step to allow a maximum nonlinear phase shift of 3 mrad, and limited to a maximum step size of 0.1 km. At each amplifier site, the signal is amplified so that the signal energy is restored to that at the input. At the output of the system, after a final amplification, the channels are filtered optically with a Bessel filter of variable order (10 in the work described here) with a bandwidth of several times the bit rate, and then electrically at baseband with a 20th-order Bessel filter typically with a bandwidth of 0.6 times the bit rate. Eye diagrams and power spectra can be plotted.

Fig. 11 shows the input spectrum for an eight-channel 10-Gb/s simulation. The laser linewidth of each channel is 10 MHz, and the channel spacing is 200 GHz. The channels are modulated with a 64-bit NRZ sequence with a modulator bandwidth of 10 GHz. Fig. 12(a) shows the output spectrum for an eight-channel system with 200-GHz channel spacing, operating at 10 Gb/s over 360 km of dispersion-shifted fiber with a 120-km amplifier spacing. The injected power is 8 dBm per channel. This power is less than that used in a

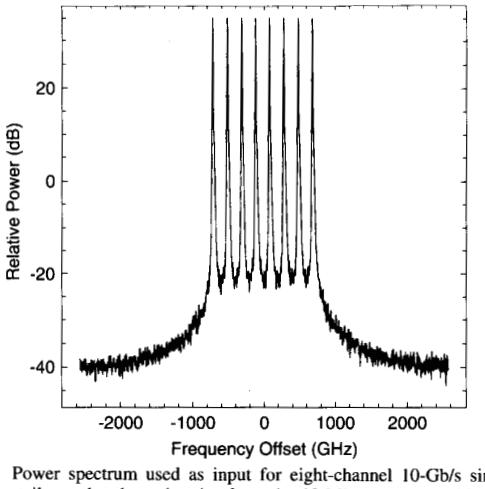

Fig. 11. Power spectrum used as input for eight-channel 10-Gb/s simulations. The tails on the channels arise from the 10-MHz laser linewidth. The channels are referred to by number from right to left.

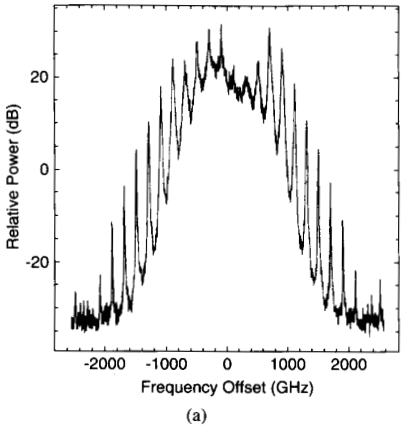

Fig. 12. (a) Output power spectrum and (b) eye pattern for channel four of an eight-channel 360-km system with 120-km amplifier spacing, each channel operating at 10 Gb/s, with input power to each span of 8 dBm per channel (average power). The transmission fiber has the zero of chromatic dispersion at the center of the channel band. The dispersion slope is 0.08 ps/nm^2 · km.

recent single-channel field experiment [21] and should be a reasonable lower bound on that required for such a system.

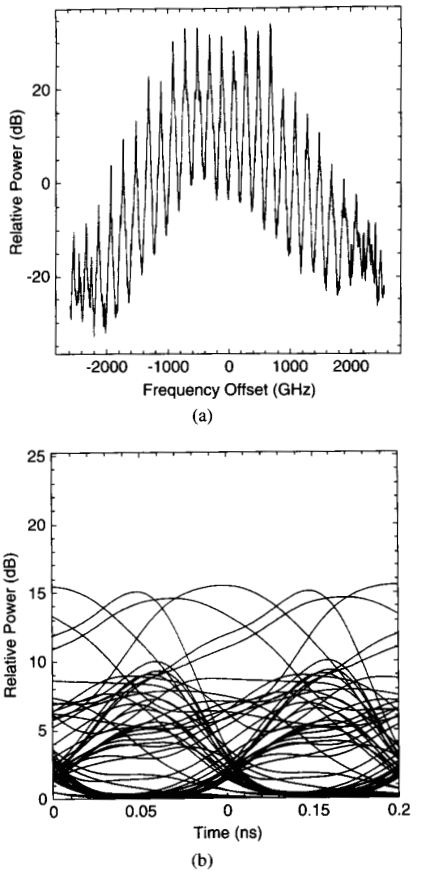

Fig. 13. Same as Fig. 12 but the transmission fiber consists of 5-km segments where the dispersion of each segment is a random sample from a Gaussian distribution with zero mean and a standard deviation of 1 ps/nm · km.

The frequency of the dispersion zero is at the center of the channel band between channels 4 and 5 (zero frequency offset). Note the proliferation of mixing products and severe depletion of some channels. Fig. 12(b) shows the eye pattern for channel 4 of this system. The eye is completely closed by the random parametric gain and loss of the various bits. This is in agreement with theoretical expectations as well as the experiment of Figs. 2–5.

There are various ways in which the variation of dispersion along the fiber line can affect this impairment. First, we will consider the effect of random variations of dispersion likely to be encountered in actual installations. Fig. 13 shows the received eye pattern and output power spectrum for the same case as Fig. 12 but with random variation of dispersion. The transmission fiber is divided into 5-km lengths and for each length a new value of dispersion is chosen from a Gaussian distribution with standard deviation of 1.0 ps/nm · km. This value of the standard deviation is much larger than one would expect from production fibers and this should magnify any improvement in the system performance. While there is some improvement in the power spectrum, the eye pattern is still quite degraded. Of course, there is substantial probability that

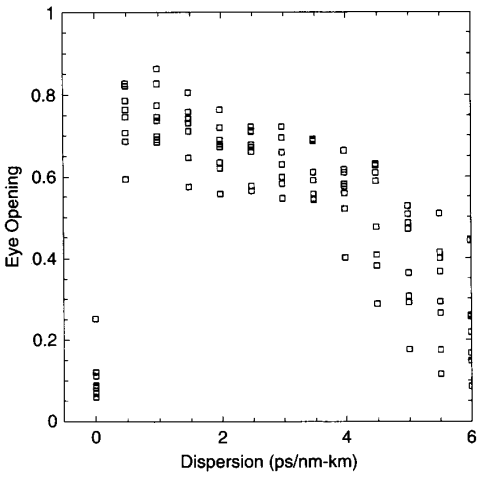

Fig. 14. Plot of fractional eye opening for each of eight channels in the system of Fig. 12 as a function of transmission line dispersion. The input power in this case is 6 dBm per channel.

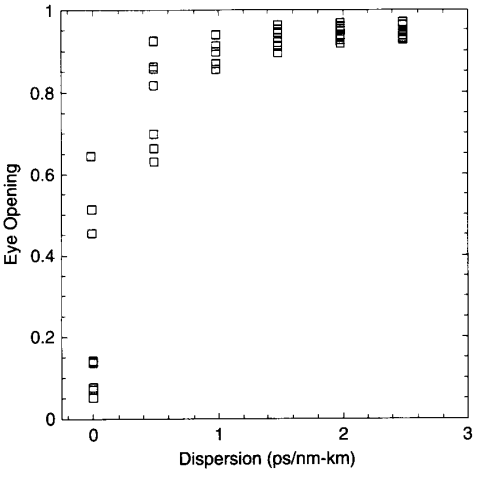

Fig. 15. Plot of fractional eye opening versus transmission line dispersion. The dispersion of the transmission fiber is compensated by a fiber with negative dispersion placed just before the amplifiers to give a net zero dispersion.

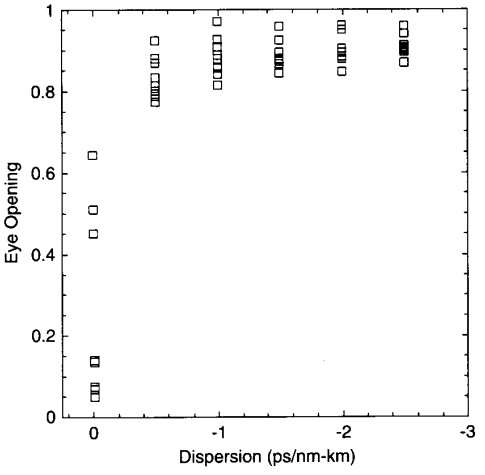

Fig. 16. Plot of fractional eye opening versus transmission line dispersion. The transmission fiber has negative dispersion and is compensated by lengths of conventional fiber placed before the amplifiers.

a particular installation will have a worst case set of dispersion values which maximizes the impairment, since the nonlinearity is particularly sensitive to the fiber near the transmitter.

Phasematched generation of mixing products can be reduced by offsetting the zero dispersion wavelength from the center of the channel band. Fig. 14 shows a plot of fractional eye opening, defined as the separation between the minimum "one" level and the maximum "zero" level divided by twice the average power, for each of the eight channels as a function of the chromatic dispersion of the transmission fiber from 0 to 6 ps/nm · km. Each channel operates at 10 Gb/s with an average power of 6 dBm. The complete degradation at zero dispersion quickly improves as the dispersion increases, but the optimum performance is achieved for a dispersion of 1 ps/nm · km and then degradation due to dispersion again closes the eye. The best performance achieved still corresponds to a 1–2 dB penalty. Compensation for the linear dispersion by fiber with negative dispersion should allow the use of transmission fiber with larger dispersion, resulting in smaller nonlinear impairments while avoiding penalties from linear dispersion. Fig. 15 shows a plot of fractional eye opening versus dispersion when the transmission fiber dispersion is compensated by fiber with negative dispersion with a magnitude 50 times that of the transmission fiber, placed before the amplifiers. (This placement of the compensating fiber avoids nonlinear effects. In actual system use the compensating fiber would be placed inside a two stage amplifier [21], but still the operating power can be kept low enough to allow linear operation.) Note that in this case the system performance improves monotonically with the dispersion of the transmission fiber. The improvement saturates when the dispersion reaches 2 ps/nm· km. For these cases with moderate dispersion values there is no discernible impairment from mixing. The residual penalties probably arise from self- or cross-phase modulation.

Similar results can be obtained with other dispersion maps. In particular, we have investigated the use of negative dispersion transmission fiber in combination with conventional fiber with 16 ps/nm · km dispersion for compensation. Fig. 16 shows the dependence of eye opening on transmission fiber dispersion in this case. Note that the behavior is similar for this case and that of Fig. 15. Both cases show rapid improvement with dispersion, which saturates after roughly 2 ps/nm · km. The differences in details are likely due to random phase differences arising from laser linewidth.

Since most deployed fiber is not dispersion-shifted, it is reasonable to consider operating with conventional fiber for transmission and using a compensating fiber with large negative dispersion. Fig. 17 shows the output eye diagram for channel four for this case. Again there is no discernible impairment from mixing. This option will become attractive when low-loss dispersion compensating fiber becomes readily available.

A fourth possible dispersion map alternates segments of positive- and negative-dispersion fibers with equal length.

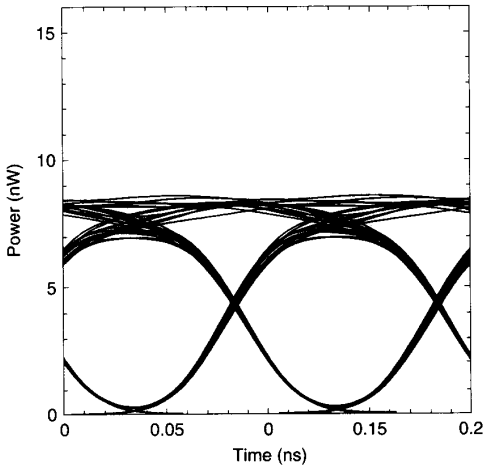

Fig. 17. Output eye diagram for channel 4 when the transmission fiber is conventional step index fiber with dispersion of 16 ps/nm · km, and core area of 80 μm^2. The compensating fiber has a dispersion of 800 ps/nm · km. The input power was 6 dBm per channel.

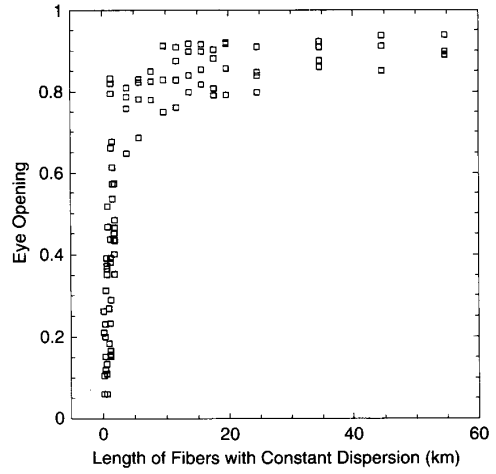

Fig. 18. Plot of fractional eye opening versus length of fibers with constant dispersion when the dispersion alternates between +2 ps/nm · km and −2 ps/nm · km. This simulation was performed for a four-channel system with 200-GHz channel spacing, and an input power of 6 dBm per channel.

We have obtained results similar to Figs. 15 and 16 for this case. An important parameter is the length scale over which the dispersion averages to zero. We consider the case where the transmission fiber is composed of lengths of fiber with dispersion equal to +2 ps/nm · km or −2 ps/nm · km. Fig. 18 shows the fractional eye opening as a function of the length of the fiber segments with constant dispersion, which is half the period of the alternation. For extremely short segment length, the fiber behaves as if it were a uniform fiber with the average, in this case zero, dispersion. As the segment length increases the four-photon mixing is suppressed. The characteristic length required to achieve low penalties corresponds to that where the phase mismatch accumulated for the mixing products becomes greater than $\approx 2\ \pi$. For a two-tone product with channels separated by 200 GHz, this length is 6.4 km. This explains the general shape of Fig. 18.

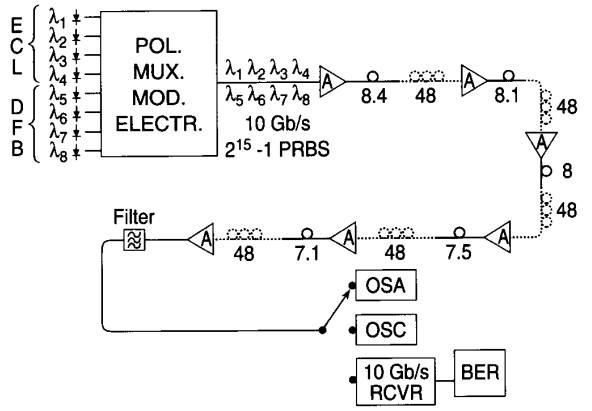

Fig. 19. Experimental diagram for eight 10-Gb/s channels transmitted over 280 km of fiber using dispersion management. The transmission fiber had a chromatic dispersion of ≈2.5 ps/nm · km and was compensated by conventional step index fiber placed just after each optical amplifier.

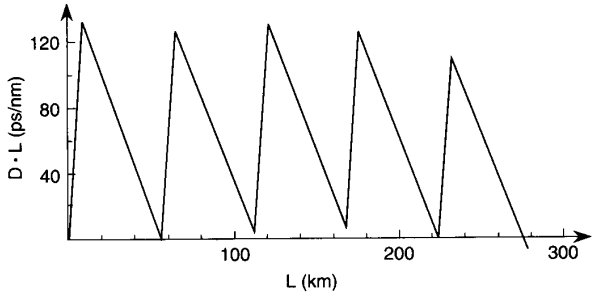

Fig. 20. Dispersion map for the experiment of Fig. 19.

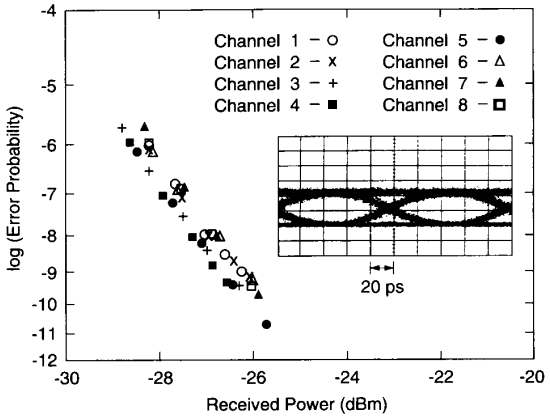

Fig. 21. Bit-error-ratio curves for the eight channels with inset eye diagram at system output.

Fig. 19 shows an experimental diagram which embodies the strategy of negative dispersion fiber compensated with conventional fiber (as in Fig. 16). In this experiment, eight 10-Gb/s channels were transmitted over 280 km consisting of 5 links comprising 50 km of fiber with dispersion of −2.5 ps/nm · km and 8 km of conventional fiber, [18]. Fig. 20 shows the dispersion map for this system. The bit error ratio performance of all eight channels is shown in Fig. 21. All channels are within 0.5 dB of the baseline. This uniform performance was

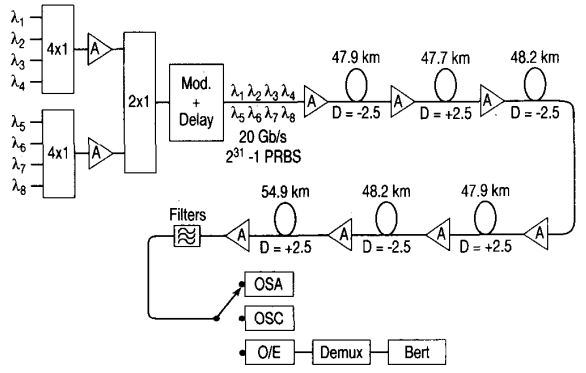

Fig. 22. Experimental diagram for transmission of eight 20-Gb/s channels over 300 km of fiber employing span-by-span dispersion reversal.

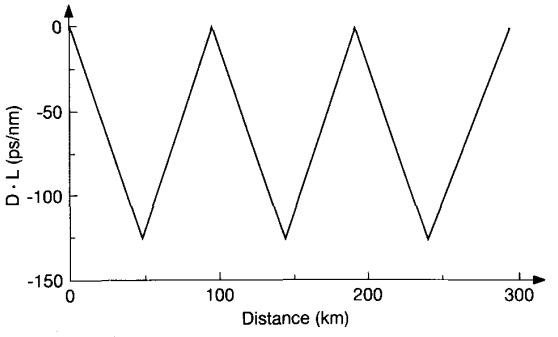

Fig. 23. Dispersion map for 8 × 20-Gb/s experiment.

achieved by using preemphasis of the transmitted power of the channels [22] to obtain equal output signal-to-noise ratios for all channels. Fig. 22 shows an experimental diagram for a system using the strategy of alternating between positive and negative dispersion with equal magnitude (as in Fig. 18). The dispersion alternated between ±2.5 ps/nm · km. The length of the fiber segments with constant dispersion was 50 km. The dispersion map of the system is shown in Fig. 23. This dispersion map was used to transmit eight 20-Gb/s channels over 300 km with 50-km amplifier spacing, [23]. The bit error ratios for all eight channels are shown in Fig. 24, again, there were no significant transmission penalties observed, although there is somewhat greater scatter in the individual channel sensitivities, arising from residual differences in the output signal-to-noise ratios. The inset in Fig. 24 shows the eye diagram of one of the channels at the system output. The degradation apparent in the eye pattern is present in the input eye pattern as well and is due to bandwidth limitations in the electronics.

Four-photon mixing presents severe limitations to wavelength multiplexed systems operating in fiber with low chromatic dispersion. However, these limitations can be ameliorated by spacing the channels unequally, ensuring that no mixing products fall on any of the channels, allowing significantly enhanced performance using conventional dispersion-shifted fiber. If it is possible to use new fiber, low total chromatic dispersion for the system may be maintained while avoiding

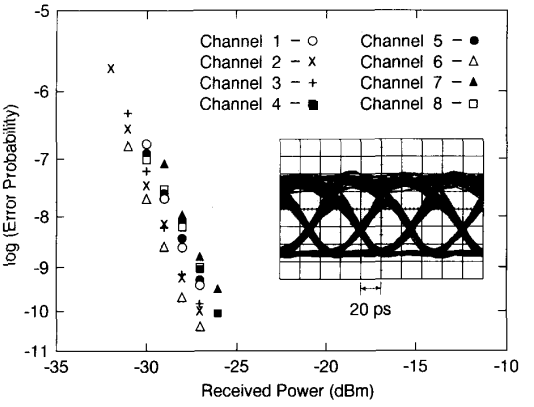

Fig. 24. Bit-error-ratio curves for the eight channels with output eye diagram (inset).

the use of any individual fibers with low dispersion, thus avoiding phasematching of the four-photon mixing process. If the magnitude of the dispersion used is sufficient, mixing products are not generated. This can be implemented with a variety of dispersion maps, including conventional fiber, with dispersion zero at 1300 nm, combined with dispersion compensation. Unequal spacing has been shown to allow a 6–7 dB increase in transmitted power and has been used to demonstrate 8 × 10-Gb/s transmission over 137 km (11 Tb · km/s) in a repeaterless configuration. The dispersion management scheme has demonstrated 48 Tb · km/s transmission of eight channels over 300 km. These strategies may be combined since their action is essentially independent, allowing further capacity increases.

REFERENCES

[1] D. Marcuse, "Derivation of analytical expressions for the bit error probability in lightwave systems with optical amplifiers," *J. Lightwave Technol.*, vol. 8, p. 1816, 1990.

[2] R. H. Stolen, "Parametric amplification and frequency conversion in optical fibers," *IEEE J. Quantum Electron.*, vol. QE-18, pp. 1062–1072, 1982.

[3] K. O. Hill, D. C. Johnson, B. S. Kawasaki, and R I. MacDonald, "CW three-wave mixing in single-mode optical fibers," *J. Appl. Phys.*, vol. 49, p. 5098, 1978.

[4] N. Shibata *et al.*, "Crosstalk due to three-wave mixing process in a coherent single-mode transmission line," *Electron. Lett.*, vol. 22, p. 675, 1986.

[5] M. W. Maeda, W. B. Sessa, W. I. Way, A. Yi-Yan, L. Curtis, R. Spicer, and R. I. Laming, "The effect of four-wave mixing in fibers on optical frequency-division multiplexed systems," *J. Lightwave Technol.*, vol. 8, p. 1402, 1990.

[6] K. Inoue and H. Toba, "Error-rate degradation due to fiber four-wave mixing in four-channel FSK direct-detection transmission," *IEEE Photon. Technol. Lett.*, vol. 3, p. 77, 1991.

[7] D. G. Schadt, T. D. Stephens, "Power limitations due to four-wave mixing effects in frequency division multiplexed coherent systems, using cascaded optical amplifiers," *J. Lightwave Technol.*, vol. 10, p. 1715, 1992.

[8] K. Inoue, "Fiber four-wave mixing suppression using two incoherent polarized lights," *J. Lightwave Technol.*, vol. 11, p. 2116, 1993.

[9] ——, "Reduction of fiber four-wave mixing influence using frequency modulation in multichannel IM/DD transmission," *IEEE Photon. Technol. Lett.*, vol. 4, p. 1301, 1992.

[10] ——, "Suppression technique for fiber four-wave mixing using optical multi-/demultiplexers and a delay line," *J. Lightwave Technol.*, vol. 11, p. 455, 1993.

[11] N. Shibata, R. P. Braun, and R. G. Waarts, "Phase-mismatch dependence of efficiency of wave generation through four-wave mixing in a single-mode optical fiber," *IEEE J. Quantum ELectron.*, vol. 7, pp. 1205–1210, 1987.

[12] K. Inoue, "Phase-mismatching characteristic of four-wave mixing in fiber lines with multistage optical amplifiers," *Opt. Lett.*, vol. 17, p. 801, 1992.

[13] D. G. Schadt, "Effect of amplifier spacing on four-wave mixing in multichannel coherent communications," *Electron. Lett.*, vol. 27, p. 1805, 1991.

[14] D. Marcuse, A. R. Chraplyvy, and R. W. Tkach, "Effect of fiber nonlinearity on long-distance transmission," *J. Lightwave Technol.*, vol. 9, p. 121, 1991.

[15] F. Forghieri, R. W. Tkach, and A. R. Chraplyvy, "Reduction of four-wave mixing crosstalk in WDM systems using unequally spaced channels," *IEEE Photon. Technol. Lett.*, vol. 6, pp. 754–756, 1994.

[16] ——, "WDM systems with unequally spaced channels," *J. Lightwave Technol.*, vol. 13, no. 5, 1995.

[17] F. Forghieri, R. W. Tkach, A. R. Chraplyvy, A. H. Gnauck, and R. M. Derosier, "Repeaterless transmission of 8 10-Gb/s channels over 137 km (11 Tb/s-km) of dispersion-shifted fiber," *IEEE Photon. Technol. Lett.*, vol. 6, pp. 1374–1376, 1994.

[18] A. R. Chraplyvy, A. H. Gnauck, R. W. Tkach, and R. M. Derosier, "8 × 10-Gb/s transmission through 280 km of dispersion-managed fiber," *IEEE Photon. Technol. Lett.*, vol. 5, pp. 1233–1235, 1993. and references therein.

[19] C. Kurtzke, "Suppression of fiber nonlinearities by appropriate dispersion management," *IEEE Photon. Technol. Lett.*, vol. 5, p. 1250, 1993.

[20] G. P. Agrawal, *Nonlinear Fiber Optics.* San Diego, CA: Academic, 1989.

[21] C. D. Chen, "Field demonstration of 10Gb/s-360km transmission through embedded standard (non-DSF) fiber cables," in *Opt. Fiber Commun. Conf. '94.*, San Jose, CA, paper PD27; and *Electron. Lett.*, vol. 30, p. 1139, 1994.

[22] A. R. Chraplyvy, J. A. Nagel, and R. W. Tkach, "Equalization in amplified WDM lightwave transmission systems," *IEEE Photon. Technol. Lett.*, vol. 4, p. 920, 1992.

[23] A. H. Gnauck, A. R. Chraplyvy, R. W. Tkach, and R. M. Derosier, "160-Gb/s (8 × 20 Gb/s WDM) 300-km Transmission with 50-km Amplifier Spacing and Span-by-Span Dispersion Reversal," in *Opt. Fiber Commun. Conf.* San Jose CA, 1994, paper PD19; and *Electron. Lett.*, vol. 30, pp. 1241–1242, 1994.

R. W. Tkach (M'84), photograph and biography not available at the time of publication.

A. R. Chraplyvy, photograph and biography not available at the time of publication.

Fabrizio Forghieri (S'89–M'93), photograph and biography not available at the time of publication.

A. H. Gnauck, photograph and biography not available at the time of publication.

R. M. Derosier, photograph and biography not available at the time of publication.